Kinetics of heterogeneous nucleation on intrinsic nucleants in pure fcc transition metals

2009 J. Phys.: Condens. Matter 21 464113

(http://iopscience.iop.org/0953-8984/21/46/464113)

IOP Publishing Journal of Physics: Condensed Matter

J. Phys.: Condens. Matter **21** (2009) 464113 (10pp) doi:10.1088/0953-8984/21/46/464113

Kinetics of heterogeneous nucleation on intrinsic nucleants in pure fcc transition metals

G Wilde[1,4], C Santhaweesuk[2], J L Sebright[3], J Bokeloh[1] and J H Perepezko[2]

[1] Institute of Materials Physics, University of Münster, Wilhelm-Klemm-Straße 10, D-48149 Münster, Germany
[2] Department of Materials Science and Engineering, University of Wisconsin-Madison, 1509 University Avenue, Madison, WI 53706, USA
[3] Caterpillar Incorporated, Advanced Materials Technology, Peoria, IL 61629, USA

E-mail: gwilde@uni-muenster.de

Received 22 April 2009, in final form 6 September 2009
Published 27 October 2009
Online at stacks.iop.org/JPhysCM/21/464113

Abstract

Nucleation during solidification is heterogeneous in nature in an overwhelmingly large fraction of all solidification events. Yet, most often the identity of the heterogeneous nucleants that initiate nucleation remains a matter of speculation. In fact, a series of dedicated experiments needs to be designed in order to verify if nucleation of the material under study is based on one type of heterogeneous nucleant and if the potency of that nucleant is constant, e.g. for a population of individual droplets, or stays constant over time, e.g. throughout repeated melting/solidification cycles. In this work it is demonstrated that one way to circumvent ambiguities and analyze nucleation kinetics under well-defined conditions experimentally is given by performing statistically significant numbers of repeated single-droplet experiments. The application of proper statistics analyses based upon a non-homogeneous Poisson process is shown to yield nucleation rates that are independent of a specific nucleation model. Based upon this approach nucleation undercooling measurements on pure Au, Cu and Ni as model materials have confirmed that the experimental strategy and analysis method are valid. The results are comparable to those obtained by classical nucleation theory applied to experimental data that has been verified to comply with the assertions that are necessary for applying this model framework. However, the results reveal also other complex nucleant–sample interactions such as an initial transient undercooling behavior and impurity removal during repeated cycling treatments. The transient undercooling behavior has been analyzed by a nucleant refining model to provide new insight on the operation of melt fluxing treatments.

(Some figures in this article are in colour only in the electronic version)

1. Introduction

The stochastic nature of the nucleation process that initiates the liquid to solid phase transformation demands measuring a statistically significant number of events for a detailed characterization of the underlying kinetics. Solitary measurements on the undercooling response, ΔT, of an individual sample do not provide the necessary information about the statistical parameters that describe the expected average value and the variance of the obtained results. Therefore, the nucleation kinetics of the liquid to solid phase transformation is most often studied on large numbers of independent nucleation events in dispersions of supposedly similar individual droplets [1]. For evaluating these data it is assumed that the kinetic parameters deduced from the behavior of a large number of nuclei measured once adequately describe the mechanisms involved in the nucleation

[4] Author to whom any correspondence should be addressed.

of a single crystallite. However, the underlying statistical principle (the Ergoden hypothesis), which states that the time average over a large number of events observed on one sub-system equals the ensemble average observed simultaneously for a large number of sub-systems, holds only for time independent events, i.e. for time-invariant nucleation rates of the individual droplets. Moreover, the statistical analysis assumes that not only the expected average undercooling value of the individual particles, but also that the moments of the obtained distribution are equal to the respective parameters describing the distribution of undercooling values obtained in multiple measurements on a single, time-invariant sample. That assumption only holds if the nucleation mechanism is fixed, i.e. if one constant type of nucleation site is uniformly distributed (seeded) throughout the droplets or without any extraneous crystalline phase for the special case of homogeneous nucleation. However, the large number of droplets (of the order of 10^6) and their small size (often about 10 μm) promote the reliability of the obtained information by averaging out the supposedly few droplets that contain nucleants of different potency.

An important application of the droplet method has been developed and applied extensively by Skripov [2, 3]. For the case of determining the maximum superheat limit for boiling of metastable liquids, the use of transparent materials allows for the ready identification of samples influenced by heterogeneous nucleants and the establishment of homogeneous nucleation conditions. The extension of this approach to the crystal nucleation onset in highly supercooled liquid metals is possible, however it is difficult to establish clear proof for the operation of homogeneous nucleation. For crystallization studies, droplet populations can be employed where heterogeneous nucleation is revealed by the freezing of a subgroup of the population at low undercooling. However, for this case the population group exhibiting the maximum undercooling cannot be taken as representing homogeneous nucleation unless detailed kinetics measurements demonstrate a dependence of the kinetics on sample volume and independence on droplet surface coating [4]. In actual fact, these stringent conditions are rarely satisfied for crystal nucleation so that heterogeneous nucleation is the operative mechanism in most undercooling studies of the liquid to solid phase transition.

Although the droplet emulsion technique has often been successfully applied to low-melting metals and alloys [4–6], it is difficult to apply at high temperatures due to the lack of carrier media that are sufficiently stable to prevent coagulation of the dispersoids. Therefore, bulk samples are usually studied in undercooling measurements on higher-melting metals and alloys. In order to achieve large undercooling values, techniques for active nucleation site removal such as fluxing in a glass slag [7–9] or melting in a reducing atmosphere [10] have to be applied.

In several ways the single drop and droplet population samples offer similar capabilities, but there are also important distinguishing features as noted in table 1. For example, for a given nucleation mode, both sample types allow for the measurement of the nucleation rate over the narrow temperature range of crystallization. The droplet population sample provides this information in a single measurement. When different catalytic sites appear in separate droplets, the action of the various sites may be difficult to resolve in droplet population samples, particularly when the potencies are similar. The single drop method provides an alternate route for probing regions of overlapping potency at the expense of multiple measurements.

Table 1. Comparison of the distinguishing features of 'multiple-droplet' and 'single-droplet' experiments.

Single run, multiple droplets	Single droplet, multiple runs
Average behavior of large number of independent nucleation events	Direct observation of individual nucleation event
Convolute nucleation statistics/multiple sites	Convolute nucleation statistics/site development
Identical thermal history for all droplets	Identical droplet for all nucleation events
Traces average behavior	Traces the most potent site in a particular droplet

In addition, special care has to be taken in the evaluation of undercooling data obtained from such repeated measurements since pronounced dependencies on the experiment time, i.e. the number of the melting/freezing treatment (cycle), and on the details concerning the experimental boundary conditions have been reported [11, 12]. Thus, the effective nucleation kinetics can change during the measurements and this invalidates a statistical analysis that uses the techniques developed for droplet population experiments. However, in the present work only cycle independent results of the measurement series are discussed with respect to nucleation kinetics. Therefore, classical nucleation theory can be used for a comparative analysis concerning the kinetics of the nucleation process.

In the following sections the discussion begins with the theoretical background necessary for the analysis of repeated nucleation undercooling cycling measurements. The analysis is applied to a detailed set of measurements on high purity Au where the examination of the stable undercooling behavior also permits a comparison to classical nucleation theory. The transient undercooling response and observations on impurity removal during thermal cycling are analyzed by a nucleant refining model that provides new insight on the effectiveness of melt fluxing treatments. The generality of the nucleant refining concept is then demonstrated by the transient undercooling response observed in Cu and Ni.

2. Theoretical background

2.1. Nucleation kinetics

The classical nucleation theory of condensed phases is based on the competition of atomic attachment to and detachment from an existing crystalline cluster [13–16]. The nucleation rate, J, is related to the undercooling level by:

$$J_i = \Omega_i \exp[-\Delta G^* f(\theta)/kT] \quad (1)$$

with $\Delta G^* = \alpha\sigma^3/\Delta G_v^2$, σ is the solid–liquid interfacial energy that was calculated here as a function of temperature according to the Spaepen model [17]. ΔG_v is the free energy change upon solidification which is related to the undercooling [9], and α is a factor that accounts for the shape of the nucleus ($\alpha = 16\pi/3$ for spherical nuclei). Ω_i is the temperature dependent prefactor that is generally defined as the product of a nucleation site density on a surface or volume basis, the number of atoms on a nucleus surface, and a liquid jump frequency. In this work, the model equation according to [18] will be applied to describe the prefactor. $f(\theta)$ is defined as the ratio of activation energies for heterogeneous and homogeneous nucleation, respectively, and k denotes Boltzmann's constant. The undercooling limit required for homogeneous nucleation of pure Au can be estimated as $\Delta T \geqslant 400$ K [18]. That value exceeds by far any reported undercooling value for Au. Therefore, only heterogeneous nucleation will be considered in the following.

According to Turnbull, the free energy difference gained during solidification (the thermodynamic 'driving force') can be approximated as $\Delta S_M \Delta T$ for pure metals. This product, where ΔS_M is the entropy of fusion, represents the first term in the Taylor-series of the actual ΔG_v-function. Therefore, this assumption is always valid for $\Delta T < 0.1 T_M$ irrespective of the material. Significant deviations occur at higher undercooling values, especially for glass-forming substances, but not for Au where this simple assumption is valid for the entire undercooling range accessible to controlled measurements [9].

According to classical nucleation theory, the prefactor for heterogeneous nucleation should be approximately 10^{22}–10^{30} cm^{-3} s^{-1}, depending on the mechanism. However, experimentally determined values commonly differ from theory by several orders of magnitude [19, 10]. In the literature, several equations for the prefactor are reported that differ with respect to the number of adjustable parameters. In this work, the equation given by [18] as:

$$\Omega_i = \frac{kT\rho_i}{3\pi a^3 \eta(T)} \tag{2}$$

was used, where ρ_i is the number of nucleation sites, a is the interatomic distance in the liquid, and η is the shear viscosity of the liquid. The temperature dependence of the viscosity of pure transition metals, with units of Pa s, can be estimated as [20]:

$$\eta(T) = 10^{-3.3} \exp\left[\frac{3.34 T_M}{T - T_{g0}}\right] \tag{3}$$

where T_{g0} is the Kauzmann [21]- or ideal glass-temperature where the entropy of undercooled liquid and crystalline gold would be equal. T_M denotes the melting temperature. Transient effects can be neglected due to the low viscosity and the small temperature dependence of the viscosity of liquid Au in the temperature range of interest.

It should be noted, that the differences between the nucleation equations given in the literature are mainly due to variations of interdependent parameters, e.g. viscosity and diffusivity, that are used for the mathematical description of the process. The physical basis for the different models is identical. Thus, equations that involve a minimum number of undetermined parameters were used here to maximize the dependence of the obtained results on the experimental data.

2.2. Transformation diagrams

Under isothermal conditions, any phase transformation can be represented by the fraction transformed as a function of time. Plotting the time required for a given fraction at different temperatures produces a time–temperature transformation (TTT) diagram. For the solidification of small single droplets, the entire sample is transformed within a few microseconds, so the time for the onset of solidification is plotted rather than the time for a given fraction. The curves are generally C-shaped due to thermodynamic limitations at high and kinetic limitations at lower temperatures. The extended times required for nucleation at low undercooling are the result of the small thermodynamic driving force, while at high undercooling, as in glass-forming melts, sluggish diffusion lengthens the transformation times. The width of the curve is inversely proportional to the activation energy and the minimum time (the so-called 'nose' of the curve) is proportional to the prefactor in equation (1) [18].

Non-isothermal undercooling experiments at different constant rates give the continuous-cooling-transformation (CCT)-curve. The CCT-curve is shifted to lower temperatures and longer times with respect to the intersection of the cooling curves with the TTT-curve, due to the fact that the nucleation rate at lower undercooling is negligible compared to J at high undercooling values. It has been shown that for low rates, the continuous-cooling-transformation behavior can be approximated as $Jvt = K(T_N)$ for volume dependent heterogeneous nucleation, where K represents a constant at the nucleation temperature, T_N, between 100 and 200 [18]. Thus, the nucleation kinetics can be approximated from such data by methods that are analogous to the treatment explained for the TTT-curve.

2.3. Statistical analysis

Isothermal experiments within the undercooling range or measurements at different cooling rates trace the respective transformation curve directly, which allows for the determination of the characteristic parameters that describe the underlying kinetics. The stochastic nature of nucleation, however, offers the possibility to obtain the same information by measuring the statistical fluctuations, i.e. the distribution of undercooling values obtained at fixed experimental conditions. Informally, if nucleation events are independent and occur randomly in time they satisfy the conditions for a Poisson process [22]. In addition, the probability of an event in each time interval, i.e. histogram bin, should be small and the number of opportunities for an event to occur should be large. The formal assumptions for a Poisson process are as follows: (1) a parameter $\lambda > 0$ exists such that for any short time interval of length Δt the probability that exactly one pulse is received is $\lambda\Delta t$. (2) The probability of more than one event in Δt is negligible. (3) The number of events in Δt is independent of the number that occurred in the previous interval. Poisson processes are frequently used

Table 2. Purity and major metallic impurities of the pure metals under study.

	Au m6N	Au m5N	Cu m5N+	Cu m3N	Ni m5N
Purity (%)	99.9999	99.999	99.9995	99.9	99.999
Impurity1[a]	Fe	Ag	Fe	Ca	Fe
Impurity2[a]	Cu	Ca	Ag	Fe	Co

[a] Impurity 1, 2 give the two metallic impurities of highest abundance.

in the analysis of biological and medical data, and can be used to model some thermodynamic transitions [23]. For a Poisson process the distribution of elapsed times between events is exponential:

$$f(t) = \lambda \exp[-\lambda t] \tag{4}$$

where λ is the average number of events per unit time (rate constant). If λ varies with time the process is called a non-homogeneous Poisson process.

The rate constant of the Poisson process is proportional to the nucleation rate. To determine the rate constants, the undercooling data are first plotted as a histogram. The rate constants are then calculated in two ways: the first method [2] uses the full width at half maximum of the undercooling distribution to determine the nucleation rate. With this method the nucleation rate can be determined only at the most probable nucleation temperature (the maximum in the histogram). With the second method, the rate constant and its variance can be determined from each histogram bin using the equations [24, 25]:

$$\lambda = \frac{1}{h}\frac{d}{(s + d/2)} \tag{5}$$

$$\mathrm{Var}(\lambda) = \frac{\lambda^2}{d}\left[1 - \frac{\lambda^2 h^2}{4}\right] \tag{6}$$

where h is the bin size, d is the number of events per bin, and s is the number of events that occur in bins of higher undercooling. The nucleation rate, J, is calculated as $J = \lambda / V\, \mathrm{d}T/\mathrm{d}t$. The second method will be used to analyze the data presented here, but it should be noted that at the most probable nucleation temperature both methods give similar results.

3. Experimental details

Materials of different purity have been used to investigate the impact of foreign impurities on the nucleation behavior. Table 2 summarizes the pure metals and their respective purities that have been used in this work. Additionally, table 2 provides the metallic impurities that were present in the materials at the highest concentrations.

For the repeated melting/solidification cycles performed in a differential thermal analyzer (DTA, Perkin-Elmer DTA-7 or Setaram Labsys TG-DSC), typically samples of about 100 mg in weight were cut from the initial wires, ultrasonically cleaned in acetone and ethanol and placed into an Al_2O_3 crucible. Additionally, pyrex glass was added in the crucible such that the glass covered the interior surface of the crucible and

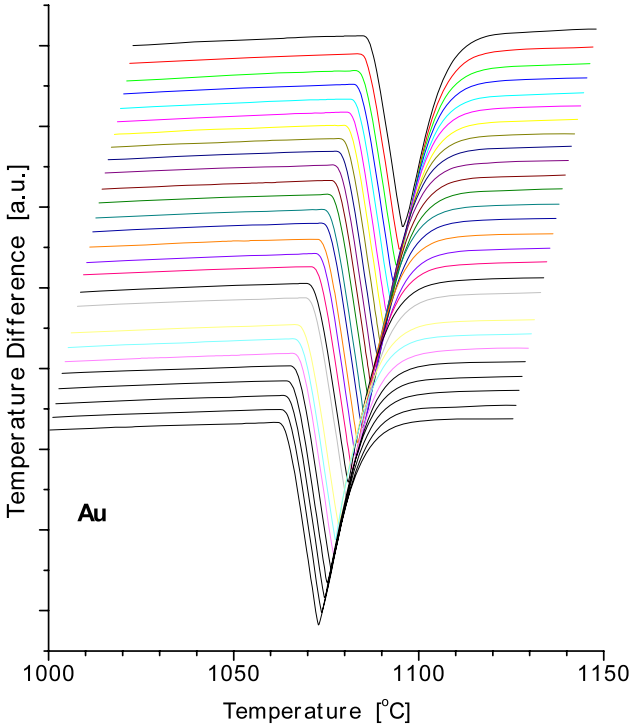

Figure 1. DTA signal of 55 subsequent melting events of the same Au sample. For clarity, only every second melting signal is shown. In order to present the experimental data more clearly, each separate curve has been shifted by a fixed offset in the directions of abscissa and ordinate, yielding the 'perspective' view introduced by the third (invisible) axis representing the cycle number of the experiment.

prevented contact between the metallic samples and the Al_2O_3 after the first heating/cooling cycle. Repeated undercooling measurements were carried out under constant gas flow at a cooling rate of 40 K min^{-1}. For most of the measurements, a Ti-getter furnace was used to purify the Ar gas (nominally 99.999% purity) from residual traces of O_2 before it entered the sample chamber. Temperature calibration of the DTA facilities were done by melting point measurements on pure metals, i.e. Al, Ag, Au and Cu, under conditions that were similar to the actual measurements. The accuracy for temperature measurement is limited by the Pt/Pt–10%Rh thermocouples to ± 1.5 K. However, the most sensitive indication for the reproducibility of the instrument was obtained from the onset temperature of the melting signal of the pure metal samples that were recorded for each melting cycle. Figure 1 presents a subset of measurements performed on pure Au of 6N purity.

The onset temperatures that were obtained from a tangent construction that is commonly used to measure the melting temperatures of pure substances varied by only 0.15 K over 55 subsequent melting cycles. During the entire set of measurements the melting temperature was monitored and periodically determined by the tangent construction. The results varied randomly within about the same confidence interval of 0.2 K. Therefore, the crystallization temperatures were determined from the DTA-curves with an accuracy of 0.1 K considering an error of ± 0.2 K.

The high growth velocity even at modest undercooling (e.g., about 2 m s^{-1} for Au at $\Delta T = 80$ K [26]) results in a

Table 3. Maximum undercooling values of Au at different cooling rates.

dT/dt (K min^{-1})	40	20	10	5	3	2	1	0.5	0.25
ΔT_{max} (K)	213.6	213.2	210.7	210.2	208.1	206.4	205.5	203.2	203.5

rapid temperature increase (i.e. 'recalescence') of the sample during crystallization. Therefore, the initial temperature increase that marks the crystallization onset measured by the DTA occurs at a higher rate than the instrumental reading of the temperature difference every 0.2 s. As a result, often crystallization occurred between two measurement readings which led to the exclusion of the actual crystallization temperature. At a given cooling rate of 40 K min^{-1}, the difference between the measured temperature of the signal onset and the crystallization temperature can vary by 0.15 K. For this reason, each of the cooling curves was inspected individually and, if necessary, the crystallization onset was determined by the intersection of extrapolated tangents to the baseline and the steepest slope of the crystallization signal.

In addition to the repeated measurements performed under identical experimental conditions that are used for the statistical analysis, further measurements were performed at different cooling rates between 0.25 and 40 K min^{-1} to determine the rate dependence of the undercooling response. Calibration experiments as described above were conducted individually for each cooling rate. Low cooling rates were used rather than rates higher than 40 K min^{-1} to retain the same accuracy as determined for the repeated measurements at a fixed rate.

4. Experimental results on pure Au

Figure 2 shows the undercooling values that were obtained under a purified Ar atmosphere during 590 melting/solidification cycles. ΔT exceeded 200 K in more than 95% of the cooling experiments after an initial 'transient' of about 25 cycles (inset in figure 2) where ΔT increased almost linearly. The minor fraction of the data at lower undercooling has no impact on the statistical analysis. In addition, experiments were performed at different cooling rates to obtain experimental information on the continuous-cooling-transformation (CCT)-curve and also for analyzing the nucleation kinetics of the system for comparison, also according to classical nucleation theory. The measurements of the undercooling response under identical conditions (figure 2) revealed a probability larger than 98% that at least one undercooling value in five successive cycles exceeds $\Delta T = 210$ K. Thus, five independent measurements have been performed for each cooling rate with $dT/dt \geqslant 1$ K min^{-1}. Measurements at lower rates were performed three times. The maximum undercooling values, ΔT_{max}, are summarized in table 3. It is important to note that other undercooling measurements [12] give values that exceed the steady-state value in figure 2 so that the current results represent a heterogeneous nucleation of crystallization.

During a discrete subset of experiments, additional quasi-isothermal annealing treatments have been performed below the equilibrium crystallization point at several temperatures

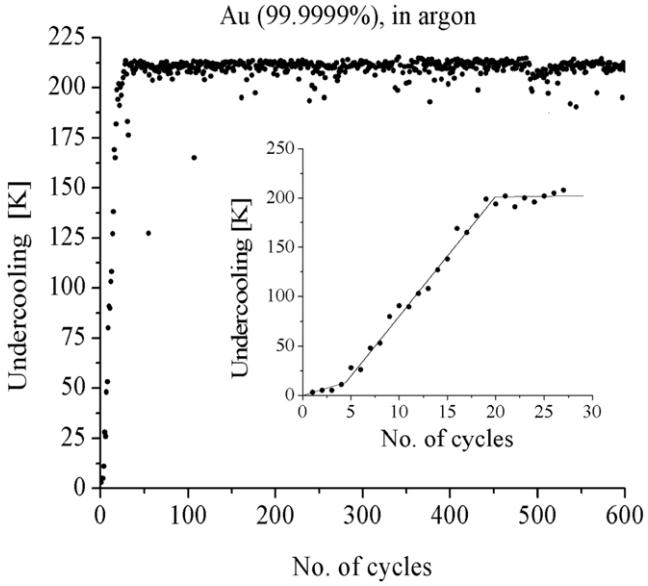

Figure 2. Undercooling values obtained on repeatedly cycling one bulk Au sample. The inset shows the initial cycle dependence.

and for different times to trace the experimental TTT-curve of the material. Initial transients of the sample temperature occurred at the onset of the holding segments that are due to the thermal momentum of the DTA device. The non-isothermal transients that surmount the programmed isothermal annealing temperatures could be minimized in principle by applying low cooling rates. Yet, a basic assumption with respect to the determination of a TTT-curve is a negligible nucleation probability prior to the isothermal annealing treatment. Thus, a rate of 40 K min^{-1} was used in most of the experiments to cool the sample down to the holding temperature. The data obtained previously at that rate indicates a negligible nucleation rate at $\Delta T < 200$ K. The resulting data shows that isothermal annealing at temperatures higher than 1150 K for up to 2100 s does not affect the nucleation behavior during the subsequent cooling runs at 40 K min^{-1}. Even multiple annealing treatments at successively lower temperatures do not alter the crystallization temperature, e.g. the sample crystallized still at $\Delta T > 205$ K after annealing for 1800 s at temperatures lower than 1193 K and subsequently for 1800 s at temperatures lower than 1159 K. In total, the sample was kept for more than 3800 s at undercooling levels in excess of 140 K without crystallization. However, if the temperature of the sample surmounted 1132 K during the transient at the beginning of the holding segment, crystallization occurred always within the first two minutes of the annealing time. From this quasi-isothermal crystallization data, i.e. from the experimental data obtained under conditions of a slow but finite rate of temperature change, the TTT-curve cannot be constructed directly because of the residual temperature

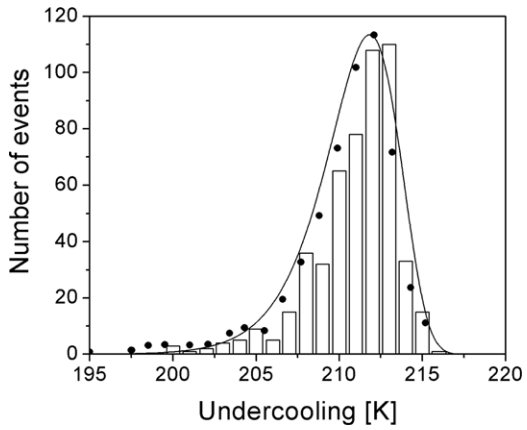

Figure 3. Histogram of 531 undercooling measurements of a 6N pure gold sample. The solid line is the best fit line from the statistical description based on equations (5) and (6). The filled circles represent the undercooling frequencies that were obtained based on an analysis of the cumulative distribution function to avoid the possible confounding influence of the bin size. This figure has been taken from [12]. Copyright 2005 by Elsevier.

change. However, for different temperatures in the transient range times can be determined that are shorter than the nucleation time corresponding to the TTT-curve.

5. Steady-state nucleation kinetics of pure Au

The initial transient behavior indicates a modification of the nucleation kinetics. This result has been discussed in detail in a separate contribution [12] and will be analyzed also in the section of this paper related to the results obtained on pure Cu and Ni. However, the current analysis focuses on the nucleation kinetics under defined conditions. A stability analysis was performed to ensure the statistical significance of the measured data set before further evaluation. For this purpose, the nucleation rate has been determined for several cycle intervals of increasing width between the cycles 30 and 480. As a result, more than 140 cycles are necessary after the initial transient to obtain a stable solution from the statistical analysis.

The resulting linear dependence indicates that a single nucleation mechanism is active throughout the 560 measurements following the initial transient. Thus, the most important assumption for classical nucleation theory is fulfilled and it is reasonable to analyze the data within the framework of classical nucleation theory. As a consistency check, the distribution function corresponding to the linear fit is displayed in figure 3 together with the experimentally obtained histogram.

Moreover, the filled circles that are additionally indicated in figure 3 correspond to the numerical derivative of the experimental undercooling data that were plotted continuously as a cumulative distribution, i.e. the filled circles correspond to the data given as

$$\delta\Delta T_n(\Delta T) = \frac{\mathrm{d}}{\mathrm{d}(\Delta T_n)}\left[\frac{\sum_{i=1}^{n}\Delta T_i}{\sum \Delta T}\right]_n. \qquad (7)$$

This alternative analysis excludes artifacts that stem from the arbitrary choice of the bin size in histogram analyses. Figure 4 indicates the impact of different choices of the bin size on the results obtained for the site density and the contact angle. It should be stressed at this point that no strict rule for defining the bin size exists. Thus, care needs to be taken if nucleation kinetics parameters are evaluated on the basis of a 'binning' analysis. In any case, since analyzing the same data on the basis of the derivative of the cumulative undercooling distribution function yields reliable results without the ambiguous choice of a bin size, this latter method should be preferred in general.

Here, a reduced subset of the data with about 1 K spacing between the data points rather than the full set of data is shown for clarity. The very good agreement between the continuous distribution function that results from the Poisson analysis and that is based on 'binning' the undercooling data, with a bin size of 1 K in this case, and the results of the cumulative distribution analysis given as filled circles indicates that the value of the bin size chosen here provides a realistic description of the undercooling statistics. The second issue concerning the applicability of the Poisson analysis is the implicit assumption that the nucleation events occur at random locations in the sample. A binomial distribution is the more appropriate model if the sample contains a small number of highly catalytic sites [22]. The experiments on highly undercooled Au presented here satisfy the conditions for the Poisson model, but this model may not be appropriate for samples with highly catalytic sites.

The third issue relates to the limits of the exponential distribution. The theoretical distribution function exists for all time values greater than zero or, correspondingly, for all temperature values less than the melting temperature during continuous cooling. In the experiments, there are temperature limits where nucleation can occur. A theoretical distribution that describes the nucleation rate for a given sample volume during continuous cooling should be finite only for temperatures between the melting temperature and the temperature for homogeneous nucleation. Attempts have been reported to formulate truncated Poisson distributions, but the resulting models are intractable [23]. For these reasons, the non-homogeneous Poisson distribution will be used here to analyze the undercooling data, although the formal assumption connected with the existence range at all temperatures lower than the melting temperature is not fulfilled.

As indicated in figure 3, the exponential distribution generally fits the histogram of the experimental data. The activation free energy and the prefactor according to equation (1) are obtained from the slope and intercept of the linear fit from the nucleation kinetics plot in figure 5(a).

The measurements at different cooling rates are evaluated similarly. A nucleation kinetics plot (figure 5(b)) summarizes the logarithm of the undercooling residence times $t_c = \Delta T/(\mathrm{d}T/\mathrm{d}t)$ in dependence of $1/T\Delta T^2$. The observed linear correlation indicates again that a single nucleation mechanism is active.

As for the Poisson analysis, the slope and the intercept of the linear fit are related to the activation free energy and

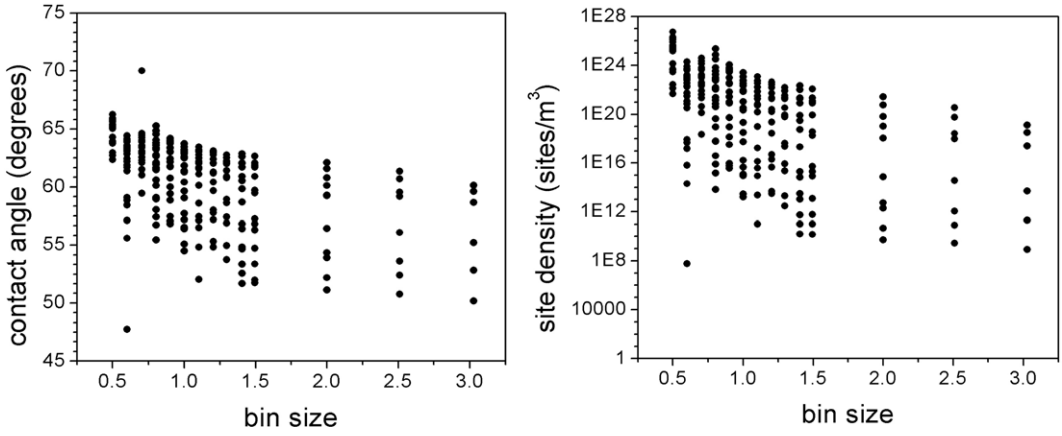

Figure 4. Variation of the obtained values for the contact angle (left) and the site density (right) upon variations of the chosen bin size.

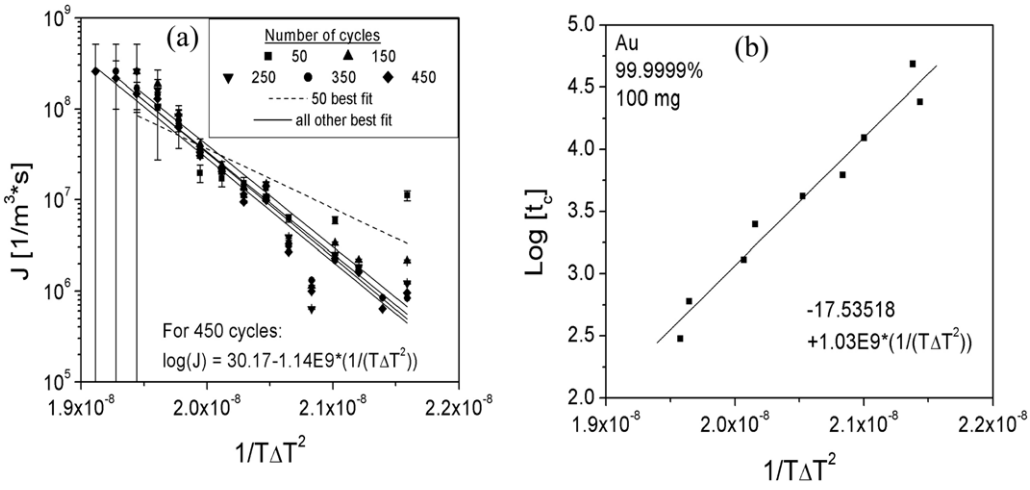

Figure 5. (a) Nucleation rates obtained from the Poisson analysis (equation (2)) of the repeated cycling experiments for increasing numbers of cycles. (b) Nucleation kinetics plot of the logarithm of the undercooling residence time as function of $1/T\Delta T^2$ for different cooling rates.

Table 4. Prefactor and activation energy for the nucleation of Au, obtained by repeated cycling and by variation of the cooling rate.

	Repeated cycling	Different cooling rates
Intercept: $\log(\Omega\ \mathrm{cm}^{-3}\ \mathrm{s}^{-1})$	32 ± 2	36 ± 2
Slope: $\Delta G^* \Delta T^2/k$ (K^3)	$(-1.2 \pm 0.2)10^9$	$(-1.1 \pm 0.2)10^9$

the prefactor, respectively if $Jvt_c = 1$ is considered. The agreement of the results obtained from the two different sets of experiments that are summarized in table 4 indicate that also the undercooling values measured at different cooling rates are characteristic for the active nucleation mechanism. The data from the two complementary sets of experiments on the same bulk sample allow for a separate calculation of the respective CCT (continuous-cooling-transformation)-curves which are close to the isothermal TTT (time–temperature transformation)-curves for slow cooling [18] according to: $Jvt = 1$. It should be noted that the underlying measurements sample the CCT-curve differently, i.e. by measuring the variance of the curve at one point (time) or by tracing the average curve over a limited time interval.

However, the transformation curves that correspond to the two measurement series coincide within the range of the accuracy and show a good agreement with the experimentally determined values as shown in figure 6. The CCT-curve obtained from the cooling rate dependent measurements has been calculated with a constant prefactor and with a temperature dependent prefactor as well. The two curves coincide completely in the experimentally accessible undercooling range.

In summary, the comparison of experiments performed at different cooling rates, experiments performed isothermally in the undercooling range and experiments conducted according to the repeated solidification approach, indicate clearly the applicability of the statistical approach that analyzes the nucleation rate on the basis of a non-homogeneous Poisson process. Moreover, the approach intrinsically enables the distinction between situations with defined and stable nucleation conditions or situations where multiple nucleants with similar potency exist that can give rise to complex dependencies on processing parameters such as overheating temperatures, soaking times, cooling rates, etc. Moreover, analyzing single samples repeatedly allows additionally

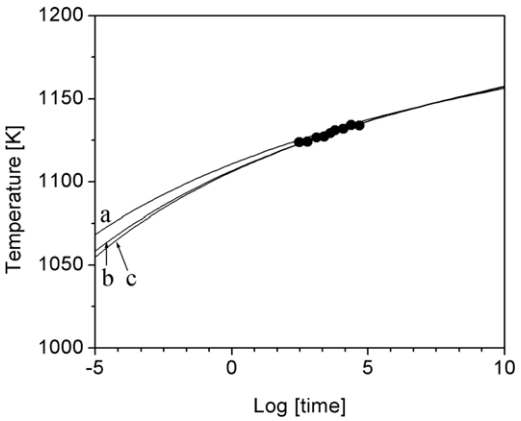

Figure 6. CCT-curves for Au obtained from parameters that were determined by repeated cycling (a) and by undercooling measurements at different rates ((b), (c)). Curves (b) and (c) are calculated with a constant prefactor and a temperature dependent prefactor, respectively. The minimum crystallization temperatures that have been obtained experimentally at different rates (and during the repeated cycling) are indicated by the full circles.

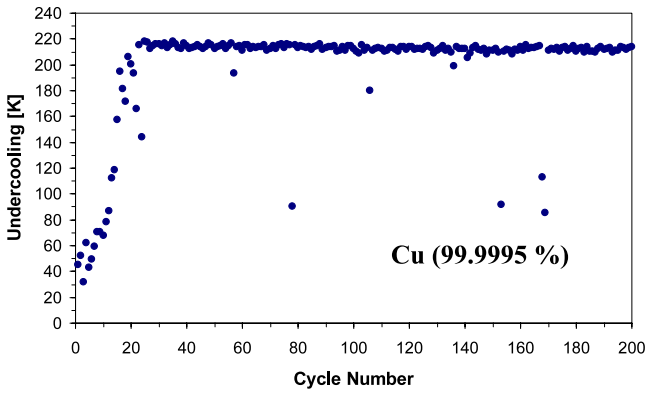

Figure 7. Undercooling response of a high purity Cu sample embedded in pyrex flux. The behavior upon repeated melting and solidification is similar to the behavior of pure Au.

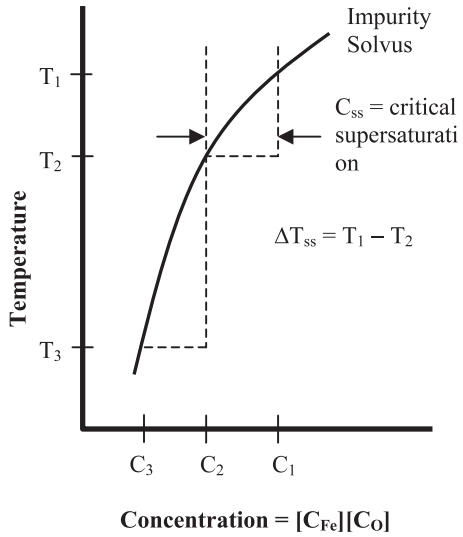

Figure 8. Schematic diagram illustrating one possible mechanism for the incremental undercooling increase using a glass flux. During each solidification cycle, the liquid surmounts the solvus and thus precipitates [Fe][O] as internal nucleants that are partially dissolved in the glass. For a constant supersaturation, C_{ss}, distinct undercooling values below the solvus must be achieved. Due to the decreasing solubility product, the undercooling for melt solidification increases, e.g. from $T_M - T_2$ to $T_M - T_3$ during the subsequent cycle.

identifying more complex nucleation scenarios, e.g. where the nucleation and subsequent solidification reaction itself affects the nucleant distribution, as indicated briefly in the following section.

6. Non-steady-state nucleation conditions: nucleant modification–nucleant precipitation

Clearly, the undercooling response measured during the initial 25 cycles on the pure Au sample (6N purity) shown in figure 3 differs considerably from the response in the following experiments where steady-state nucleation conditions were attained. In order to obtain information on the underlying 'cleaning' or 'de-nucleation' mechanism, series of experiments with well-controlled measurement parameter variations (maximum overheating temperature, soaking time, oxygen partial pressure in the gas environment, glass coverage of the sample within the crucible) have been conducted. As a result, a model has been proposed that is based on the precipitation of an internal nucleant phase through the reaction of metallic impurities in solution in the melt with constituents of the gas environment of the sample [12]. According to measurements of the residual resistivity ratio performed on the Au sample before and after repeated solidification cycling and with regard to measurements of the Kondo effect in Au of similar nominal starting purity [27], a simplified description can be put forward based on Fe and O as the constituents that precipitate as [Fe][O]-nucleant. Due to the presence of Pyrex glass as a fluxing medium that has a high solubility for metal oxides, oxide dispersoids that can act as internal nucleants are taken out of the system at a finite probability, yielding a net cleansing upon repeated cycling [12].

In order to test the validity of this model approach, repeated solidification cycling experiments have also been performed on pure Cu of different purity [28] and on pure Ni. For these pure fcc metals, the formation of oxides of the material under study must also be included into the considerations, in contrast to the studies on pure Au. Yet, the results of repeated solidification cycling experiments e.g. for Cu of 5N+ starting nominal purity (99.9995% purity) shown in figure 7 indicate similar behavior as observed for high purity Au (inset of figure 3).

The explanation of the undercooling increase as a function of cycle number is given in detail in [12] and is schematically shown in figure 8. Basically, a minimum free enthalpy difference ΔG_V must act as chemical driving force to nucleate the precipitation of the nucleant phase. ΔG_V is given as:

$$\Delta G_V = RT_2 \ln(C_{ss}) = \frac{-\Delta H_s \Delta T_{ss}}{T_1}. \qquad (8)$$

The respective terms are explained in the caption of figure 8. After precipitation, the undercooled melt can easily nucleate

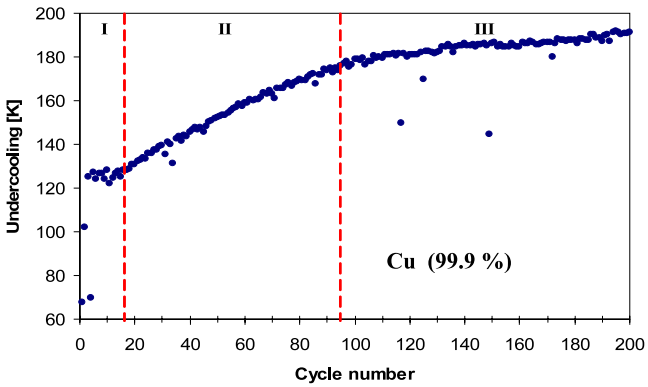

Figure 9. Undercooling response upon repeated solidification cycling of a Cu sample of low purity (99.9%). Three intervals of the undercooling transient with distinct slopes are indicated.

heterogeneously on these intrinsic nucleants that are at least partially dissolved in the glass flux, according to the model. Thus, in order to build up a comparable driving force for precipitation in the subsequent solidification cycle, the undercooling below the [Fe][O] solvus must be comparable.

Therefore, the absolute temperature for precipitation decreases, yielding higher undercooling of the melt solidification, since the solubility product decreases. In fact, the experimental data of the cycle dependent undercooling can be used for calculating impurity solvus curves that are consistent with the nucleant refinement model [12, 28]. With material of lower purity or in situations where the probability for internal oxidation is higher, the situation might become more complex: for Cu of 3N purity an extended undercooling transient was observed that extended for more than 200 repeated cycles. Interestingly, the undercooling transient consisted of three intervals with distinct slopes (figure 9).

Microstructure investigations confirmed the correlation of the first transient interval with the primary formation of CuO: at small cycle numbers, clear CuO dendrites were observed within the sample volume. However, at higher cycle numbers (i.e. within the subsequent interval of cycle numbers that displayed a different slope) no CuO phase was observed within the sample after solidification from the undercooled melt (figure 10). Similarly, for pure Ni (99.995% purity) cycle dependent undercooling values were observed that varied similarly as the amount of NiO formed at high temperatures [29]. These observations are in line with the nucleant refinement model proposed in [12] and emphasize the importance of the intrinsic impurities that are present in any real-world material. The findings also indicate the importance of the control of the processing parameters including the sample environment, especially in cases such as bulk glass formation where large undercooling values are mandatory.

7. Conclusions

Repeated undercooling measurements on the same bulk sample have shown that a time-invariant nucleant distribution can be achieved for pure Au. The analysis of statistically significant numbers of nucleation events under steady-state nucleation conditions, based on describing nucleation as a non-homogeneous Poisson process, yielded similar values for the nucleation kinetics parameters as obtained from experiments that were conducted in a more conventional way, i.e. at different cooling rates. The good agreement of the results from the two different sets of experiments shows that the statistical method is well suited to evaluate the parameters that describe the nucleation process, given that a defined nucleation state of the sample has been achieved. Moreover, this approach allows a more detailed investigation of complex couplings between nucleation, growth and processing parameters, as indicated by the nucleant refinement behavior during initial solidification cycling. In combination with atomistic models of the heterogeneous nucleation process, these parameters can further be used to determine values for the solid–liquid interfacial energy and other kinetics parameters from experimentally obtained data.

Acknowledgment

The financial support of DFG within the SPP 1296 is gratefully acknowledged.

References

[1] Vonnegut B 1948 *J. Colloid Sci.* **3** 563
[2] Skripov V P 1977 *Crystal Growth and Material* ed E K Scheel and H J Scheel (Amsterdam: North-Holland) p 328

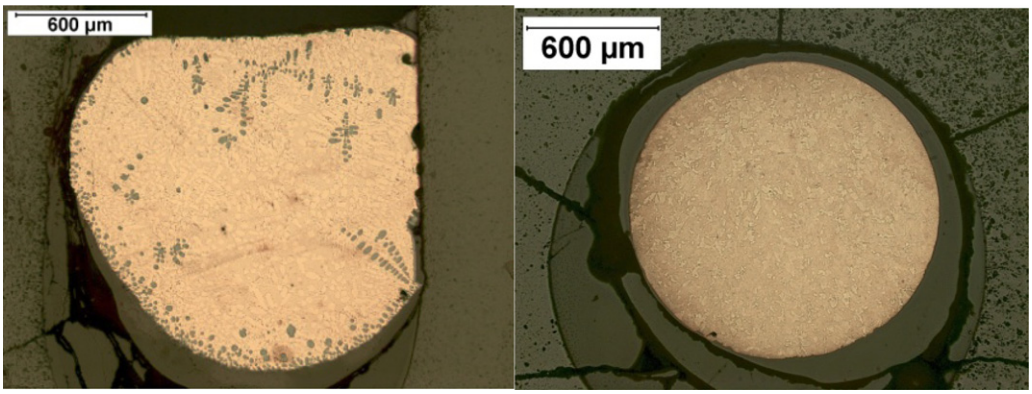

Figure 10. (Left) Optical micrograph of Cu (99.9%) after solidification at $\Delta T = 30$ K and after the initial cycles at $\Delta T = 143$ K (right).

[3] Skripov V P 1974 *Metastable Liquids* (New York: Wiley)
[4] Turnbull D 1952 *J. Chem. Phys.* **20** 411
[5] Turnbull D and Cech R E 1950 *J. Appl. Phys.* **21** 804
[6] Perepezko J H 1984 *Mater. Sci. Eng.* **65** 125
[7] Bardenheuer P and and Bleckmann R 1939 *KWI Eisenforsch.* **21** 201
[8] Wilde G, Görler G P, Willnecker R and Dietz G 1994 *Appl. Phys. Lett.* **65** 397
[9] Wilde G, Mitsch C, Görler G P and Willnecker R 1996 *J. Non-Cryst. Solids* **205–207** 425
[10] Herlach D M 1994 *Mater. Sci. Eng.* R **12** 177
[11] Bradshaw F J, Gasper M E and Pearson S 1958–59 *J. Inst. Met.* **87** 15
[12] Wilde G, Sebright J L and Perepezko J H 2006 *Acta Mater.* **54** 4759
[13] Becker R and Döring W 1935 *Ann. Phys., Lpz.* **24** 719
[14] Turnbull D and Fisher J C 1949 *J. Chem. Phys.* **17** 71
[15] Chalmers B 1954 *Trans. AIME* **200** 519
[16] Jackson A and Chalmers B 1956 *Can. J. Phys.* **34** 473
[17] Spaepen F 1994 *Solid State Phys.* **47** 1
[18] Boettinger W J and Perepezko J H 1993 *Rapidly Solidified Alloys* ed H H Liebermann (New York: Dekker) chapter 2
[19] Turnbull D 1981 *Prog. Mater. Sci.* **Chalmers Ann Vol** 269
[20] Iida T and Guthrie R I L 1988 *The Physical Properties of Liquid Metals* (Oxford: Clarendon)
[21] Kauzmann W 1948 *Chem. Rev.* **43** 219
[22] Yost F G 1974 *J. Cryst. Growth* **23** 137
[23] Consul P C 1989 *Generalized Poisson Distributions: Properties and Applications* (New York: Dekker)
[24] Gehan E A 1969 *J. Chronic Dis.* **21** 629
[25] Uttormark M J, Zanter J W and Perepezko J H 1977 *J. Cryst. Growth* **177** 258
[26] Hoyt J J and Asta M 2002 *Phys. Rev.* B **65** 214106
[27] Svoboda P 1978 *J. Phys. F: Met. Phys.* **8** 1757
[28] Santhaweesuk C and Perepezko J H 2009 at press
[29] Bokeloh J and Wilde G 2009 at press